



Received 05th June 2020,
Revised 17th July 2020,
Accepted 09th August 2020

[DOI: 10.14456/past.2020.2](https://doi.org/10.14456/past.2020.2)

The Variation of Superconducting Critical Temperature of the Mn₃O₄ Doped- and Mn₃O₄ Composited-Y145 Superconductor

Anongdavone Ponchanthai^{1*}, Tunyanop Nilkamjon¹, Supphadate Sujinmaparm^{2,3}, Thitipong Krauehong⁴, Somporn Tiyasri⁵, Wirat Wongphakdee⁵ and Pongkaew Udomsamuthirun¹

¹ *Prasarnmit Physics Research Unit, Department of Physics, Faculty of Science, Srinakharinwirot University, Bangkok, 10110, Thailand.*

² *Department of Physics, Faculty of Liberal Art and Science, Kasetsart University, Khamphaeng Saen Campus, Nakhon Pathom, 73140, Thailand.*

³ *Thailand Center of Excellence in Physics (ThEP), Bangkok, 10400, Thailand.*

⁴ *Department of Physics, Faculty of Science and Technology, Suratthani Rajabhat University, Surat Thani, 84100, Thailand.*

⁵ *Department of Chemistry, Faculty of Science, Srinakharinwirot University, Bangkok, 10110, Thailand.*

*E-mail: anongttc@gmail.com

Abstract

The Y145 superconductors modified with manganese oxide (Mn₃O₄) were synthesized via the solid-state reaction by using the Mn₃O₄ with various concentrations of dopant. Our research focused on the investigations of the physical and structural properties in the doping materials and the composite materials preparations. The SEM and EDX were determined the surfaces of materials and the identifications of elements. The XRD patterns were indicated for the microstructure of these samples. The critical temperature (T_c) of the samples was measured by the four-point probe resistivity measurements. The Cu²⁺, Cu³⁺, and oxygen content were investigated by Iodometric titration. The results revealed that the influence of different concentrations of Mn₃O₄ was significantly on the increase of the T_c as increasing the Mn content in both processes. The SEM and ERD showed that the grain size of the doping samples changed slightly in comparison with the composite samples in most samples. The XRD demonstrated that the crystal structure was in the orthorhombicity. The Iodometric titration indicated that the ratio of Cu³⁺/Cu²⁺ depended on the T_c, which was rather linear dependence. The increase of T_c with increasing concentrations of Mn₃O₄ could be due to the hole filling in the CuO₂ planes.

Keywords: Superconductor, Y145 doped with Manganese Oxide, Critical temperature, Solid-state reaction.

1. Introduction

The discovery of the YBa₂Cu₃O_y (Y123) ceramic superconductor (1), the Y123 showed the critical temperature at 92 K. In 2010, the YBa₂Cu₃O_y family modified the compound samples with several compositions (2). Next year, the YBa₄Cu₅O_y (Y145) superconductor (3), found that the critical temperature onset of Y145 at 94 K. Many researchers reported that The Y145 superconductor was synthesized some properties of YBa_mCu_{1+m}O_y (m = 2,3,4,5) (4) superconductor by using the calcination temperature was at 1223 K and varied the sintering temperature was at 1223 K and 1253 K, the T_c onset of Y145 was 91 K.

However, the research has consistently shown that the preparation and characterization of

Y123 and Y₂Ba₃Cu₅O_y (Y235) superconductors (5) doped with fluorine, showed that the critical temperature was 92 K - 95 K. The influence of doped materials has greatly been explored by many researchers such as the effect of the physical properties of superconductors, the Ti doping on structural and superconducting properties of the Y123 high-T_c superconductor was done (6). More studies were done to support that the effect of magnetic and nonmagnetic nano metal oxides doping on the critical temperature of the YBCO superconductor (7). It noted that the Y123 doped with nano metal oxide of Mn₃O₄ with 0.2 wt% were synthesized by solid-state reaction technique, the critical temperature onset of Y123 at 112 K for Y123 + 0.2 wt%Mn₃O₄. In some case, the Mn₃O₄ doping on the superconductor

samples of $Y123 + xMn_3O_4$ with increasing of concentrations ($x = 0.1, 0.2, 0.3, 0.4$ and 0.5wt\%) of nano metal oxides (8), reported that the physical properties of all samples mostly were unchanged in samples and exhibited large grain size with the presence of pores between the grains. One showed that the Mn_3O_4 was distributed over the surfaces and the orthorhombic structure.

Besides, the research efforts (9) reported the oxygen content effected the critical temperature of $Y145$, the Ag doping on $Y145$ superconductor with the determination of Cu^{2+} and Cu^{3+} in the oxygen content found that the relation on the amount of Cu^{2+} and Cu^{3+} , the Cu^{3+}/Cu^{2+} ratio of $Y145$ were high amount on Ag-doped sample. The present work aimed to investigate the variation of the superconducting critical temperature of the Mn_3O_4 doped and Mn_3O_4 composited $Y145$ superconductor with different concentrations of Mn_3O_4 on some physical properties. The crystal structures of samples were investigated by using X-ray diffraction (XRD). The surfaces of materials were considered by the scanning electron microscopy (SEM). The identifications of the compositions of different elements in the specific samples were determined by using the energy-dispersive X-ray spectroscopy (EDX). The Iodometric titration was used to determine the amount of Cu^{2+} , Cu^{3+} , and oxygen content. The resistivity measurements and the critical temperature were measured by using the four-point probe technique.

2. Materials and Experiment

The $YBa_4Cu_5O_y$ ($Y145$) superconductor doping and compositing on Mn_3O_4 with the different concentrations were synthesized by solid-state reaction technique. The high-purity (99.99%) raw materials of Y_2O_3 , $BaCO_3$, CuO , and Mn_3O_4 powders were mixed, ground, and reacted according to the calculations of the chemical formula in two processes. The doping materials were prepared by starting the various concentrations of precursor powders (Y_2O_3 , $BaCO_3$, CuO , and Mn_3O_4), which were the pure sample of $YBa_4Cu_5O_y$ superconductor and the doped samples of $YBa_4Cu_5Mn_{0.015}O_y$, $YBa_4Cu_5Mn_{0.030}O_y$, and $YBa_4Cu_5Mn_{0.060}O_y$ superconductors with (0.005, 0.010, and 0.015 Mole) Mn_3O_4 . Consequently, the composite materials were prepared by the raw materials of Y_2O_3 , $BaCO_3$, and CuO in the desired atomic ratio as 1:4:5, as $YBa_4Cu_5O_y$ superconductor, which was composited with xMn_3O_4 where $x = 0.005, 0.010$, and 0.015 Mole, as $Y145$, $Y145 + 0.005Mn_3O_4$, $Y145 + 0.010Mn_3O_4$, and $Y145 + 0.015Mn_3O_4$, respectively. The calcination process was done at 1223 K for 24 hours in the powder form. All samples were pressed into pellets and took into the sintering process at 1223 K for 24 hours and the annealing process is at 823 K for 24 hours in the air.

The physical properties were analysed by the resistivity measurements (10), which was set as a function of temperature in a range of 77-120 K by using liquid nitrogen and measured by a standard D.C four-point probe technique (11). All obtained samples were characterized by SEM micrograph and EDX (JEOL JSM-6610LV) analysis (12) was carried out to investigate stoichiometry and chemical composition. The XRD patterns (Bruker D8-Discover); the crystal structures were performed by Rietveld full-profile analysis method. Finally, the oxygen content (13, 14) was characterized by Iodometric titration technique. This titration was carried out by determining the amount of Cu^{2+} , Cu^{3+} , and oxygen content. The oxygen content was calculated by using the sum of the oxygen number of all samples. The $YBa_4Cu_5O_y$ superconductors were the samples of nonstoichiometric compounds in which the oxygen content is variable. The coefficient Y in the formula had noninteger value in the range of 10.5-11.

3. Results and Discussion

The surface morphology and elemental compositions of all samples were demonstrated by SEM and EDX in JEOL (JSM-6610LV). The SEM of all samples in the doping and composite materials with different concentrations of Mn_3O_4 was used for power magnifications of 2000 ($10.\mu\text{m}$). From Figure 1, the surface morphology changes with the addition of the Mn_3O_4 in the system. The grain size of the $Y145$ doped with Mn_3O_4 samples presented the clear of small grain over the surface with random alignment distribution. Moreover, the grain size of the doped sample was better compared to the pure sample and the composite materials samples. According to the SEM results, the surface morphology and average crystallite size were found to raise with increasing the Mn addition in the range $1 - 6.\mu\text{m}$. Figure 2, depicted the average grain size in all samples rather, being the same as most samples and the samples exhibited large grains randomly oriented in all directions with the presence of pores between the grains. For the composite of Mn_3O_4 , showed that Mn_3O_4 were distributed randomly over the $Y145$ grains mostly. The EDX analysis was found that the elements of all samples with Y , Ba , Cu , O , and Mn were the different values and without impurity. When computing the formula ratio by defining Yttrium to be 1, according to the chemical formula of $Y145$. Next, the elemental analysis of the superconductors samples was randomly analyzed by calculating the average in five positions over the surface samples as shown in Figures 3 and 4. The ratio of Ba , Cu , O , and Mn were shown in the following in Table 1. From EDX analysis, each of Mn_3O_4 was mostly distributed over the entire surface of the granules as pointed in a range of micron. However, the amount of 0.005 Mn_3O_4 in two processes was undetectable with the value of Mn addition in some positions.

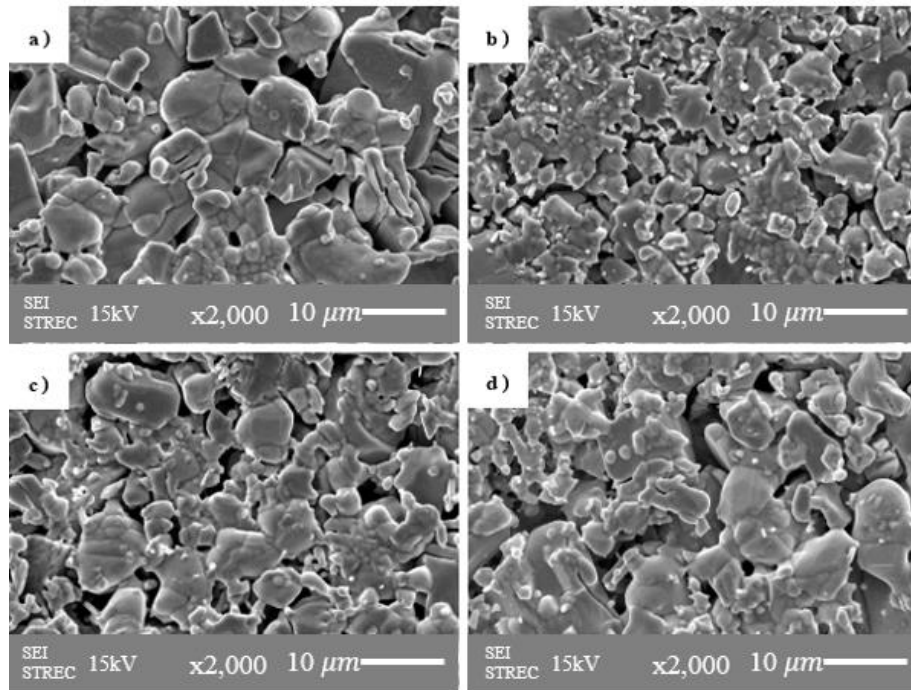


Figure 1 The SEM micrographs of samples a) $\text{YBa}_4\text{Cu}_5\text{O}_y$, b) $\text{YBa}_4\text{Cu}_5\text{Mn}_{0.015}\text{O}_y$, c) $\text{YBa}_4\text{Cu}_5\text{Mn}_{0.030}\text{O}_y$, and d) $\text{YBa}_4\text{Cu}_5\text{Mn}_{0.060}\text{O}_y$ in the doping materials (D).

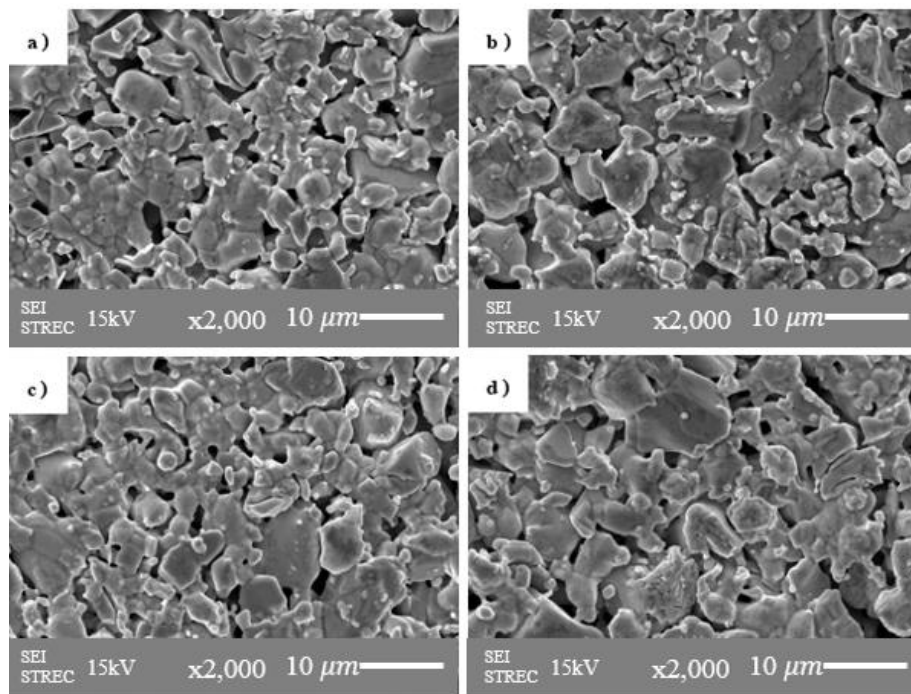


Figure 2 The SEM micrographs of samples a) Y145, b) Y145 + 0.005 Mn_3O_4 , c) Y145 + 0.010 Mn_3O_4 , and d) Y145 + 0.015 Mn_3O_4 in the composite materials (C).

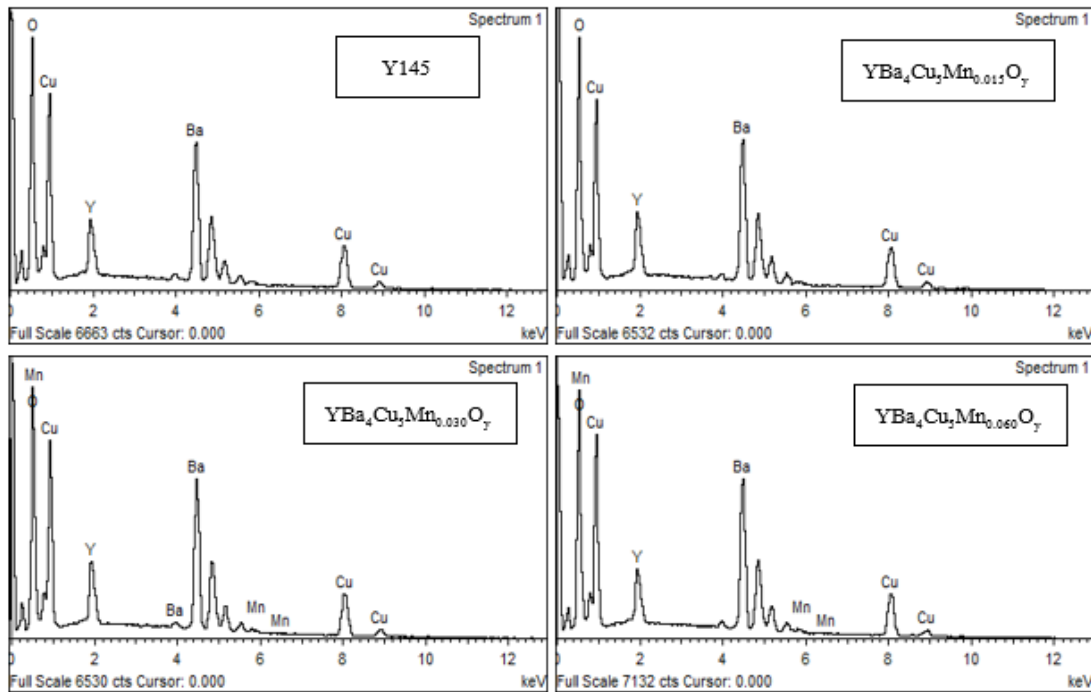


Figure 3. The EDX results of the doping materials (D).

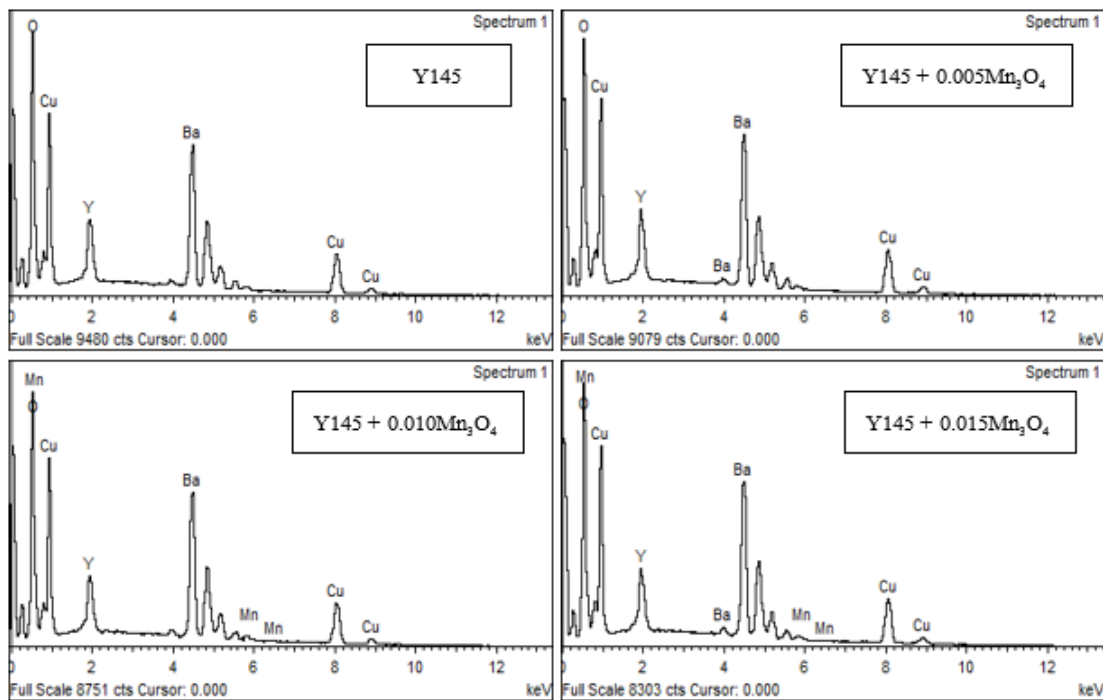


Figure 4 The EDX results of the composite materials (C).

Table 1 The ratio of elements in comparison with yttrium.

Samples	Yttrium	Barium	Copper	Oxygen	Manganese
Y145 (D)	1	3.81	5.19	13.36	-
YBa ₄ Cu ₅ Mn _{0.015} O _y	1	3.39	4.28	11.25	0.00
YBa ₄ Cu ₅ Mn _{0.030} O _y	1	3.84	5.11	12.29	0.01
YBa ₄ Cu ₅ Mn _{0.060} O _y	1	4.16	5.43	12.94	0.04
Y145 (C)	1	4.30	5.37	15.11	-
Y145 + 0.005Mn ₃ O ₄	1	3.91	4.58	12.52	0.00
Y145 + 0.010Mn ₃ O ₄	1	4.70	5.89	14.93	0.08
Y145 + 0.015Mn ₃ O ₄	1	4.80	6.00	14.91	0.10

We have two preparation processes; the doping materials and the compositing materials process, with different concentrations of Mn₃O₄. Figure 5, shows the relation between the normalized resistivity versus temperature of both processes, presenting the critical temperature of all samples. Table 2, we also found that the two processes with different concentrations can enhance the critical temperature that the highest critical temperature onset at 101 for YBa₄Cu₅Mn_{0.060}O_y and 97 K for Y145 + 0.015Mn₃O₄ samples, respectively. These results of magnetic micro metal oxides doping on structure and electrical properties of Y145 superconductors were consistent with the research of Salama et.al studied that the influence of magnetic nano metal oxides, in the doped with Mn₃O₄ increasing T_c significantly. In Table 2 also shows the difference of T_c onset and T_c offset depending on the porous surface morphology, and doping and compositing concentrations of samples.

In Figure 5, the comparison of two processes on the critical temperature is shown. So, we concluded that the critical temperature depends on the resistivity for Y145 doped and composited samples with different concentrations of Mn₃O₄. Generally, all samples showed metallic behavior in the normal state and superconducting parameters. It was also known that the doping materials process is a higher critical temperature than the compositing materials process. The value of T_c onset at 101 K, increased significantly in the doping materials process. While the process of the composite materials shows slightly critical temperature in the value of T_c onset at 97 K. The effect of two processes and concentrations on the critical temperature onset were demonstrated. The

YBa₄Cu₅Mn_{0.060}O_y had the highest critical temperature onset at 101K in the doping materials process and the Y145 + 0.015Mn₃O₄ had the highest critical temperature onset at 97 K in the compositing materials process. These represented that the increase of concentrations illustrates the effect on critical temperature indirectly that increases the oxygen content and the Cu³⁺/Cu²⁺ ratio of all samples. Additionally, the increase of T_c with doping and compositing nominal concentration confirmed that Cu atoms in the Y145 crystal lattice could be partially substituted. Some differences in T_c onset increase in comparison with pure Y145 might be caused by the solidification process as well as the formation of secondary phases rich in doping and compositing. For the Mn₃O₄ doping and compositing, we realized that there was an increase in transition temperature up to 0.015 Mole, due to the Mn inclusion, which reduced the formation of other phases and enhances the formation of Y145. However, the decrease in T_c with Mn content at 0.010 Mole indicated that Mn ions were incorporated into the Y145 structure, resulting in some changes in the microstructure and chemical properties of CuO₂ planes. Moreover, the possible Copper-pair breaking effect of magnetic ions was known to depress the transition temperature through the short-range exchange scattering.

It convinced that the value of the residual resistivity oscillates, the increasing and the decreasing value of resistivity trended in the value of zero-resistance critical temperature. It indicated that the connectivity between grains decreases gradually with increasing the doping and compositing concentration of all oxides. These effects occurred by increasing inhomogeneities in the inter-granular regions.

Table 2 The variation of normal state and superconducting parameter in all samples.

Samples	TC offset (K)	TC onset(K)	ΔT (K)	ρ(mΩ.cm)
Y145 (D)	89	92	3	39.5
YBa ₄ Cu ₅ Mn _{0.015} O _y	88	97	9	20.5
YBa ₄ Cu ₅ Mn _{0.030} O _y	88	95	7	32.2
YBa ₄ Cu ₅ Mn _{0.060} O _y	92	101	9	43.3
Y145(C)	84	91	7	18.7
Y145 + 0.005Mn ₃ O ₄	91	95	4	51.5
Y145 + 0.010Mn ₃ O ₄	88	92	4	12.7
Y145 + 0.015Mn ₃ O ₄	88	97	9	13.3

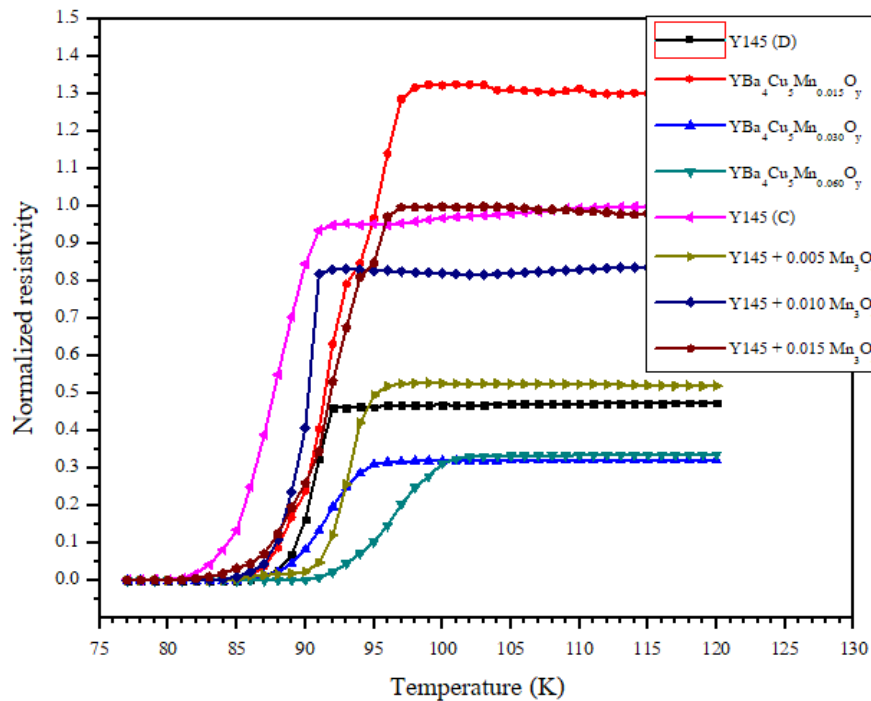


Figure 5 The normalized resistivity versus temperature of samples.

For the powder X-ray diffraction analysis, the pellets were reground to a fine powder and the XRD patterns analysis was investigated. The XRD patterns, carried out at room temperature in $2\theta = 10^\circ$ - 90° range as shown in Figure 6. The characteristic peaks of all samples; the Y145, $\text{YBa}_4\text{Cu}_5\text{Mn}_{0.015}\text{O}_y$, $\text{YBa}_4\text{Cu}_5\text{Mn}_{0.030}\text{O}_y$, $\text{YBa}_4\text{Cu}_5\text{Mn}_{0.060}\text{O}_y$ in the doping materials process and the Y145, Y145 + 0.005Mn₃O₄, Y145 + 0.010Mn₃O₄, Y145 + 0.015Mn₃O₄ in the compositing materials process, determined and compared with the research of Chainok et.al, the peaks of all samples were indicated a predominantly single-phase perovskite structure Y145 with orthorhombic symmetry and small quantities of secondary phases. When the peaks of all samples were compared with the peak of Y123 for the investigation of crystal structure (15). It mentioned that these peaks corresponding to the peak of Y123, detected by X-ray diffraction analysis. Thus, all samples were in the orthorhombic structure.

The Iodometric titration (16), investigated to determine the amount of Cu²⁺, Cu³⁺, and oxygen content. The oxygen content O_y was calculated by using the sum of the oxidation numbers of all samples, we defined that $y = 11-x$, where x is the deficiency of samples. The Cu³⁺/Cu²⁺ ratio, oxygen content, and the deficiency of all samples were indicated in Table 3. For investigating all samples, it

reported that the $\text{YBa}_4\text{Cu}_5\text{Mn}_{0.060}\text{O}_y$ showed the highest Cu³⁺/Cu²⁺, the critical temperature, and the lowest percentage of deficiency. The effect of two processes and oxygen deficiency on the critical temperature onset was shown. The relation of these parameters was almost linear dependence. It also knew that oxygen deficiency was a small value, being contributed to the increase of the critical temperature such as the highest deficiency of Y145 with a smaller critical temperature. So, we believed that the critical temperature is inversely proportional to the increment of oxygen deficiency. The ratio of Cu³⁺/Cu²⁺ versus the critical temperature onset of all samples was shown in Figure 7, it indicated that the ratio of Cu³⁺/Cu²⁺ depending on the critical temperature, with nearly the linear dependence. The $\text{YBa}_4\text{Cu}_5\text{Mn}_{0.060}\text{O}_y$ had the maximum Cu³⁺/Cu²⁺ of and the Y145 had the minimum that agrees with the highest T_c onset of $\text{YBa}_4\text{Cu}_5\text{Mn}_{0.060}\text{O}_y$ and the lowest T_c onset of Y145. Therefore, these results were consistent with the research of Supadanaison et. al. that studied the determination of Cu²⁺ and Cu³⁺ by Iodometric titration in the Y145 superconductor found that the higher the Cu³⁺/Cu²⁺ ratio was, the higher the critical temperature became. It also indicated that the $\text{YBa}_4\text{Cu}_5\text{Mn}_{0.060}\text{O}_{10.954}$ has the highest Cu³⁺/Cu²⁺ ratio at 0.222 and the highest T_c onset at 101 K. While the $\text{YBa}_4\text{Cu}_5\text{Mn}_{0.015}\text{O}_{10.863}$ has the lowest Cu³⁺/Cu²⁺ ratio at 0.170 and the T_c onset at 92 K.

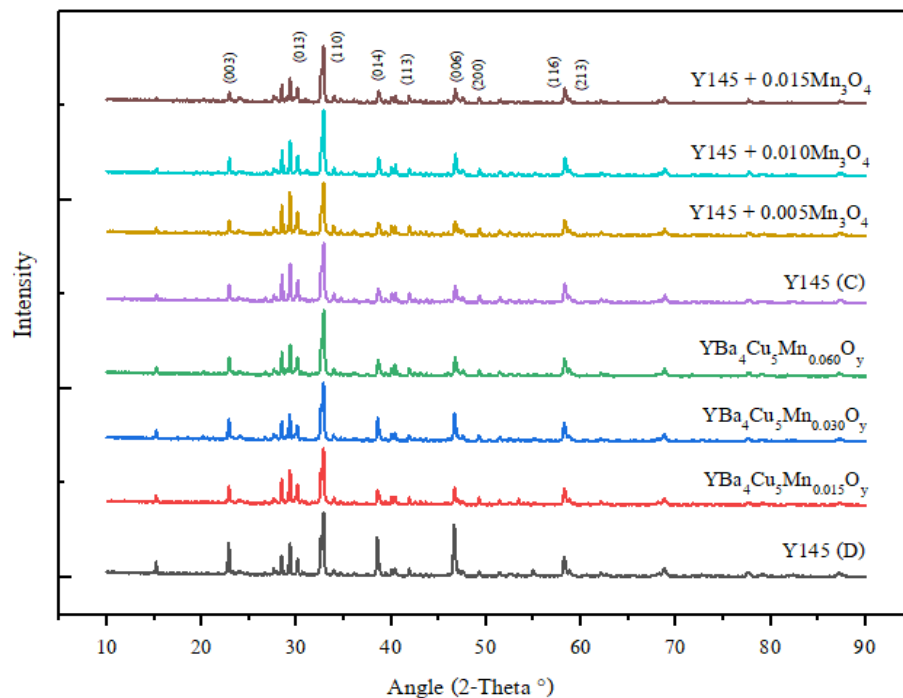


Figure 6 The X-ray diffraction patterns of samples in the doping materials and the composite materials process.

Table 3 The oxygen content and deficiency of samples.

Compounds	Cu ³⁺ /Cu ²⁺	Oxygen (O _y)	Deficiency (%)
Y145 (D)	0.170	10.863	1.249
YBa ₄ Cu ₅ Mn _{0.015} O _y	0.202	10.921	0.719
YBa ₄ Cu ₅ Mn _{0.030} O _y	0.193	10.904	0.870
YBa ₄ Cu ₅ Mn _{0.060} O _y	0.222	10.954	0.417
Y145(C)	0.173	10.869	1.188
Y145 + 0.005Mn ₃ O ₄	0.201	10.919	0.740
Y145 + 0.010Mn ₃ O ₄	0.180	10.881	1.077
Y145 + 0.015Mn ₃ O ₄	0.217	10.946	0.491

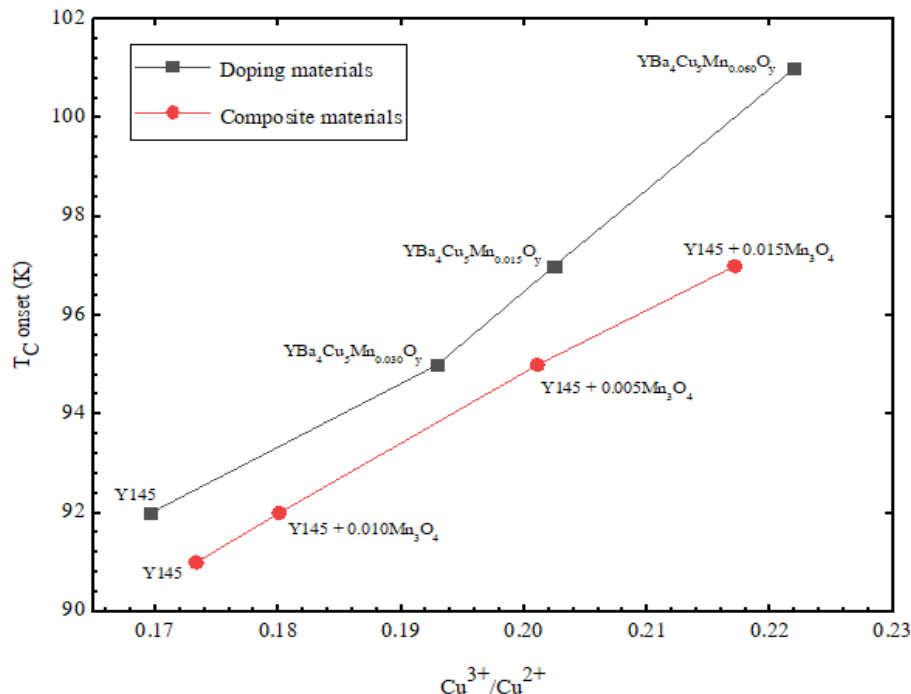


Figure 7 The ratio of $\text{Cu}^{3+}/\text{Cu}^{2+}$ versus the critical temperature onset.

4. Conclusions

The Y145 superconductors doped and composited materials with Mn_3O_4 concentrations of $x = 0.005, 0.010, 0.015$, typically synthesized by solid-state reaction. We found that the T_c onset of the doping materials process of Y145, $\text{YBa}_4\text{Cu}_5\text{Mn}_{0.015}\text{O}_y$, $\text{YBa}_4\text{Cu}_5\text{Mn}_{0.030}\text{O}_y$, $\text{YBa}_4\text{Cu}_5\text{Mn}_{0.060}\text{O}_y$ were 92 K, 97 K, 95 K, and 101 K, respectively. The composite materials process of Y145, $\text{Y145} + 0.005\text{Mn}_3\text{O}_4$, $\text{Y145} + 0.010\text{Mn}_3\text{O}_4$, $\text{Y145} + 0.015\text{Mn}_3\text{O}_4$ were 91 K, 95 K, 92 K, and 97 K, respectively. The doping and compositing with Mn_3O_4 were increased T_c significantly, it might be lead to the inclusion of Mn in the Y145 structure and enhanced the formation of Y145 with high orthorhombicity and high superconducting properties (3, 8). Also, the amount of $\text{Cu}^{3+}/\text{Cu}^{2+}$ ratio in the superconductors contributed to becoming the crystal structure of the superconductor. Therefore, the higher the $\text{Cu}^{3+}/\text{Cu}^{2+}$ ratio was, the higher the superconducting transition temperature changed. Particularly, the increase of $\text{Cu}^{3+}/\text{Cu}^{2+}$ was related to the decrease and increase of the oxygen content and the critical temperature of samples. Hence, the effect of increasing Mn content in the Y145 superconductors was equivalent to that of enhancing $\text{Cu}^{3+}/\text{Cu}^{2+}$ and the rising of the critical temperature.

Acknowledgements

The authors are exceedingly grateful to the financial support of the center, Department of Physics, Faculty of Science, Srinakharinwirot University. And the Thailand International Cooperation Agency (TICA).

Declaration of conflicting interests

The authors declared that they have no conflicts of interest in the research, authorship, and this article's publication.

References

1. Wu MK, Ashburn JR, Torg CJ, Hor PH, Meng RL, Gao L. Superconductivity at 93 K in a new mixed-phase Yb-Ba-Cu-O compound system at ambient pressure. *Phys. Rev. Lett.* 1987;58: 908-10.
2. Udomsamuthirun P, Krauehong T, Nilkamjon T, Ratreng S. The New Superconductors of $\text{YBa}_2\text{Cu}_3\text{O}_7$ Materials. *J. Supercond. Nov. Magn.* 2010;23:1377-80.
3. Chainok P, Sujinnapram S, Nilkamjon T, Ratreng S, Kritcharoen K, Butsingkorn P. The preparation and characterization of Y145 superconductor. *J. Adv. Mater. Res.* 2013;770: 295-8.
4. Chainok P, Khuntak T, Sujinnapram S, Tiyasri S, Wongphakdee W, Krauehong T. Some properties of $\text{YBa}_m\text{Cu}_{1+m}\text{O}_y$ ($m = 2, 3, 4, 5$) superconductors. *Int. J. Mod. Phys. B.* 2015;29: 1550060-6.
5. Khuntak T, Chainok P, Sujinnapram S, Nilkamjon T, Ratreng S, Udomsamuthirun P. The preparation and characterization of Y235 superconductor and Y235 doped fluorine. *J. Adv. Mater. Res.* 2014;979:228-31.
6. Sahoo M, Behera D. Effect of Ti doping on structural and superconducting property of

YBa₂Cu₃O_{7-x} high T_c superconductor. *J. Supercond. Nov. Magn.* 2014;27:83-93.

- 7. Salama AH, El-Hofy M, Rammah YS, Elkhatib M. Effect of magnetic and nonmagnetic nano metal oxides doping on the critical temperature of a YBCO superconductor. *Adv. Nat. Sci: Nanosci. Nanotechnol.* 2015;6:045013-7.
- 8. Salama AH, El-Hofy M, Rammah YS, Elkhatib M. The influence of magnetic nano metal oxides doping on structure and electrical properties of YBCO superconductor. *Adv. Nat. Sci: Nanosci. Nanotechnol.* 2016;7:015011-8.
- 9. Supadanaison R, Panklang T, Wanichayanan C, Kaewkao A, Nilkamjon T, Udomsamuthirun P. Determination of Cu²⁺ and Cu³⁺ by titration in Y134 and Y145 superconductor. *Mater. Today: Proc.* 2018;5:14896-900.
- 10. Murase S, Itoh K, Wada H, Noto K, Kimura Y, Tanaka Y. Critical temperature measurement method of composite superconductors. *Physica C Supercond.* 2001;357: 1197-200.
- 11. Da Luz M, Dos Santos C, Shigue C, De Carvalho Jr F, Machado A. The van der Pauw method of measurements in high-T_c superconductors. *Mater. Sci-Poland.* 2009;27: 569-579.
- 12. Sharma RG, Superconductivity. : Springer; 2015.
- 13. Choy JH, Choi SY, Byeon SH, Chun SH, Hong ST, Jung DY. Determination of the Copper Valency and the Oxygen Deficiency in the High T_c Superconductor, YBa₂Cu₃O_{7-y}. *Bull. Korean Chem. Soc.* 1988;9:289-91.
- 14. Harris DC, Hewston TA. Determination of Cu³⁺ Cu²⁺ ratio in the superconductor YBa₂Cu₃O_{8-x}. *J. Solid State Chem.* 1987;69:182-5.
- 15. Kruaehong T, Sujinnapram S, Udomsamuthirun P, Nilkamjon T, Ratreng S. The effect of ti-doped on the structure of Y134 and Y257 superconductors. *CAST.* 2018;18:126-32.
- 16. Harris DC, Hills ME, Hewston TA. Preparation, iodometric analysis, and classroom demonstration of superconductivity in YBa₂Cu₃O_{8-x}. *J. Chem. Educ.* 1987;64:847-50.